ELSEVIER

Journal of Contaminant Hydrology 46 (2000) 319–338

JOURNAL OF Contaminant Hydrology

www.elsevier.com/locate/jconhyd

Multicomponent transport of major cations predicted from binary adsorption experiments

Andreas Voegelin [a], Vijay M. Vulava [b], Florian Kuhnen [a], Ruben Kretzschmar [a,*]

[a] *Institute of Terrestrial Ecology, Swiss Federal Institute of Technology, Grabenstrasse 3, CH-8952 Schlieren, Switzerland*

[b] *Savannah River Ecology Laboratory, University of Georgia, Aiken, SC 29802, USA*

Received 10 December 1999; received in revised form 27 April 2000; accepted 6 July 2000

Abstract

Accurate modeling of multicomponent sorption and transport of major cations in subsurface porous media is a prerequisite for predicting complex environmental processes, such as the movement of trace metals in soils and aquifers. In this study, various cation exchange models were compared in their ability to predict ternary Ca–Mg–Na transport in an acidic soil from binary Ca, Mg, and Na adsorption data. A flow-through reactor technique was used to measure binary adsorption isotherms of Ca, Mg, and Na over wide concentration ranges of the adsorptive and the respective background cations. High-resolution transport experiments were conducted in water-saturated chromatographic glass columns. Three sorption models based on cation exchange equations were compared: a 1-site Gaines–Thomas (1-GT), a 1-site Rothmund–Kornfeld (1-RK), and a 3-site Gaines–Thomas (3-GT) model. Although the fit of adsorption data was clearly improved from the 1-GT to the 1-RK to the 3-GT model, transport predictions were overall not improved compared to the 1-GT model. While predictions by the 1-GT and the 3-GT model were virtually identical, predictions by the 1-RK model were partly improved and partly deteriorated. The most simple 1-GT model, therefore, seems to be adequate for predicting multicomponent transport phenomena involving major cations, however, multi-site models may be useful for predicting transport of trace metals in the presence of several major cations. Regardless of the

* Corresponding author. Tel.: +41-1-6336003; fax: +41-1-6331118.
E-mail address: kretzschmar@ito.umnw.ethz.ch (R. Kretzschmar).

PII: S0169-7722(00)00132-7

model used, accurate determination of the cation exchange capacity at the pH conditions of interest is extremely critical in cation transport modeling.

Keywords: Cation exchange; Reactive transport; Competitive sorption; Column technique; Modeling; Seawater intrusion

1. Introduction

Understanding the reactive transport behavior of inorganic chemical species becomes necessary when dealing with environmental problems such as fresh- or seawater intrusions into aquifers, landfill leaching plumes, or transport of heavy metals in soils and aquifers. Predicting the transport of reactive solutes in porous media generally requires both an accurate description of sorption and an appropriate transport model (Jury and Flühler, 1992). In the case of a single component adsorbing to the soil matrix, retention can be estimated from a simple batch adsorption experiment. However, in the case of a multicomponent system with several interacting species, complex coupled breakthrough patterns can arise. Such multicomponent transport phenomena can only be described with models accounting for the underlying chemical reactions between the soil matrix and the interacting solute species. For practical reasons, it is infeasible to experimentally determine the partition behavior of all species in a multicomponent system at all possible solution compositions. Therefore, the complex multicomponent system must be predicted from a limited number of simplified adsorption experiments, e.g., binary adsorption experiments with only two interacting species present at a time.

One example for multicomponent behavior is the sorption and transport of major cations (e.g., Ca^{2+}, Mg^{2+}, Na^{+}, K^{+}) in natural subsurface environments. The classical way to treat the competitive sorption of major cations is the definition of cation exchange reactions with constant exchange stoichiometry based on charge equivalents, e.g., the Gaines–Thomas convention (McBride, 1994; Sparks, 1995). Complex breakthrough patterns are reported for laboratory column and field scale experiments (Appelo et al., 1990; Beekman and Appelo, 1990; Bjerg and Christensen, 1993; Cernik et al., 1996; Dance and Reardon, 1983; Valocchi et al., 1981). Respective cation exchange coefficients were determined from binary column (Beekman and Appelo, 1990; Cernik et al., 1996) or binary batch experiments (Bjerg and Christensen, 1993), from multicomponent batch experiments (Valocchi et al., 1981), or from the composition of soil solution and exchanger phase in the field system (Dance and Reardon, 1983). However, problems can arise when using such exchange coefficients to predict cation behavior over a wide range in solution composition. Exchange coefficients may vary with solution and exchanger phase composition due to dependence on pH, ionic strength, sorbent heterogeneity, specific adsorption, or variation of the activity of the adsorbed species (McBride, 1994; Sparks, 1995). One possible approach to handle the variability of exchange coefficients would be the use of a more flexible exchange convention such as the Rothmund–Kornfeld formulation of the Gaines–Thomas exchange equation (Bond, 1995; Bond and Verburg, 1997) or the introduction of concentration dependent

acitivity coefficients for adsorbed species. An alternative approach is the introduction of additional sorption sites with different exchange coefficients, thereby accounting for chemical heterogeneity and specific adsorption in an empirical fashion (Cernik et al., 1996). For a binary Ca–Na soil system, this multi-site approach was recently shown to improve the fits of adsorption data spanning over wide ranges in solution composition (Vulava et al., 2000).

In the present study, a large set of binary adsorption data including all possible combinations within the ternary Ca–Mg–Na soil system was measured using a flow-through reactor technique. A 1-site Gaines–Thomas (1-GT), a 1-site Rothmund–Kornfeld (1-RK), and a 3-site Gaines–Thomas (3-GT) model were compared in their ability to describe the entire dataset. All three models were then coupled to a mixing-cell transport code and ternary cation transport in packed soil columns was predicted. Predictions were compared with results from high-resolution column transport experiments.

2. Materials and methods

2.1. Soil material

The soil material used in the experiments was collected from the B-horizon (15–25 cm sampling depth) of an acidic soil in northern Switzerland (Riedhof soil, aquic dystric Eutrochrept, silt loam texture). The soil material was gently broken into small aggregates, dried at 40°C, and sieved to various fractions smaller than 2 mm. For all adsorption and column experiments, the sieve fraction 63–400 μm was used. This fraction consisted of 37% sand, 47% silt, and 16% clay. It contained 6 g/kg organic carbon, and had pH 4.1 when suspended in deionized water. Exchangeable cations were determined from an unbuffered 0.1 M $BaCl_2$ extraction (Hendershot and Duquette, 1986). A potassium chloride method (Thomas, 1982) was used to measure the exchangeable acidity. From these results, a cation exchange capacity (CEC) of 0.060 ± 0.002 mol_c/kg (base saturation $\sim 20\%$) was calculated. From a 0.01-M $Ca(NO_3)_2$–$Mg(NO_3)_2$ column exchange experiment at pH 4.6, the same CEC was obtained.

2.2. Binary cation adsorption experiments

Competitive adsorption experiments were conducted in binary cation systems (Ca–Na; Mg–Na; Mg–Ca) at pH near 4.6. The solution concentrations of the respective *adsorptive cation* ranged from 10^{-7} to 10^{-1} M, while the concentrations of the respective *background cation* ranged from 0.02 to 0.5 M for Na and from 10^{-4} to 10^{-2} M for Ca and Mg. The experiments were carried out using a flow-through reactor technique (Grolimund et al., 1995). Briefly, pre-weighed soil samples were placed on cellulose–acetate membrane filters (0.45 μm, Schleicher and Schuell) in flow-through reactor cells consisting of slightly modified air monitoring cassettes. All cells were connected to a 24-channel peristaltic pump and the soil samples were extensively

pre-conditioned by leaching with 500 ml/g soil of 0.5 M $CaCl_2$, 0.5 M $MgCl_2$ or 1.0 M NaCl at a rate of 3 ml/min. The pH value of all influent solutions was adjusted to pH 4.6 by addition of HCl. Following this first pre-washing step, during which the soil was completely saturated with the respective background cation, the influent electrolyte concentration was reduced to the desired background cation concentration. After equilibrium was reached, the reactors were drained and weighed to determine the amounts of entrapped electrolyte solution. The reactors were then refilled with a solution containing the same background electrolyte plus a known amount of the desired adsorptive cation (Ca, Mg, or Na). In this adsorption step, the cell outflow was connected back to the inflow (closed-loop arrangement) and the solution was re-circulated through the reactor cells for 24 h. After equilibration, cation concentrations were measured in initial and final solutions by atomic absorption (Varian SpectrAA 400 Flame-AAS) and emission (Varian Liberty 200 ICP-AES) spectroscopy. The adsorbed amounts were calculated from differences between initial and final solution concentrations and soil weights. In order to be able to accurately measure adsorption isotherms over several orders of magnitude in adsorptive cation concentration, the soil-to-solution ratio in each reactor had to be varied from 50 to 1000 g/l. Thereby, distribution fractions of the adsorptive cation between 0.2 and 0.8 were obtained, allowing reliable estimates of the adsorbed amounts as a function of adsorptive cation in solution. Note, that varying the ratio between the soil in the reactor and the circulating solution does not alter the soil-to-solution ratio in the reactor itself, where the cation exchange reactions take place. Changing the soil-to-solution ratio in the flow-though reactor technique therefore should not affect the experimental results.

2.3. Ternary cation transport experiments

Transport experiments were conducted in ternary cation systems (Ca–Mg–Na) using a packed soil column technique. Chromatographic glass columns (Omni) were uniformly packed with the dry soil material and flushed for several minutes with CO_2 gas to displace the air from the pore space. The columns were then connected to a HPLC pump (Jasco PU-980) and pre-conditioned by leaching with several hundred pore volumes of 0.5 M $CaCl_2$ solution adjusted to pH 4.6. Solutions were first passed through a degasser (Gastorr GT-103) and then through the soil columns in the upward direction. Due to rapid dissolution of CO_2 gas, complete water saturation was achieved within a few pore volumes. Two different column dimensions were used for transport experiments. The first column (C1) was 48.1 cm long and had 0.3 cm inner diameter, while the second column (C2) was 19.1 cm long and had 0.66 cm inner diameter. These dimensions were chosen for two reasons: (i) to maximize the column Péclet number resulting in high precision, high resolution breakthrough data with well-resolved cation transport fronts, (ii) column diameter was varied to increase the range in pore water velocities (v) that could be achieved with the HPLC pump. To characterize the soil columns, a short nitrate pulse (0.1 ml) was injected and the resulting breakthrough peaks were monitored on-line using an UV–VIS detector. Pore volume, dispersivity, and column Péclet number were determined numerically from the flow rate and the first or second moments of the nitrate breakthrough curves. The column parameters are listed in Table 1.

Table 1
Properties of the two soil columns C1 and C2 used for ternary cation transport experiments

Column	C1	C2
Diameter (cm)	0.3	0.66
Length (cm)	48.1	19.1
Volume (ml)	3.46	6.53
Mass of soil (g)	4.10	7.47
Pore volume (ml)	2.11	3.87
Bulk density (g/ml)[a]	1.94	1.93
Porosity (%)	61	59
Dispersivity (mm)	~1	~1
Péclet number	~450	~250

[a]Mass of soil per pore volume.

For cation transport experiments, sequences of electrolyte solutions of varying composition were passed through the soil columns and the effluent cation concentrations were monitored. The effluents were sampled in regular intervals using an automated fraction collector. Concentrations of Ca, Mg, and Na in the effluents were measured by atomic absorption spectrometry (Varian SpectrAA 400 Flame-AAS).

Six different transport experiments were conducted, for which the sequences of feed solutions, column dimensions, and flow velocity are given in Table 2. In Experiments 1 and 2, the same sequence of feed solutions was used, but the column dimensions and flow velocity were different. The feed solution was switched three times after steady state had been reached. In Experiment 3, the Na concentration in the feed solutions was increased about 20-fold compared to Experiments 1 and 2, resulting in higher Na saturation of the soil material. In Experiments 4 and 5, the feed solution was switched before steady state had been reached. To test for possible kinetic effects on cation breakthrough, Experiment 5 was run at about 30 times lower pore water velocity compared to Experiment 4. In Experiment 6, an exchange between seawater and freshwater was mimicked with respect to typical concentrations of Ca, Mg, and Na in seawater and freshwater.

2.4. Modeling cation adsorption and transport

The competitive sorption of major cations in soils is usually described by cation exchange reactions (McBride, 1994; Sparks, 1995). Several different conventions have been proposed in the past to formulate mass action laws for cation exchange. In this study, we use the well-known cation exchange convention of Gaines and Thomas (1953). Exchange reactions in the ternary Ca^{2+}–Mg^{2+}–Na^{+} system are written as:

$$CaX_2 + 2Na^+ \leftrightarrows 2NaX + Ca^{2+} \quad (1)$$

$$CaX_2 + Mg^{2+} \leftrightarrows MgX_2 + Ca^{2+} \quad (2)$$

where X denotes an exchange site with charge -1. The activities of adsorbed species are assumed to correspond to the charge equivalent fractions y_M:

$$y_M = z_M q_M / CEC \quad (3)$$

Table 2
Sequences of feed solutions and pore water velocities applied in the ternary cation transport experiments (Experiments 1–6)

Experiment no., column, pore water velocity v (cm/min)	Influent (pore volumes)	$CaCl_2$ (mM)	$MgCl_2$ (mM)	NaCl (mM)
Experiment 1, column C1, $v = 5.6$	< 0	5.2	4.55	4.65
	0	5.3	–	–
	20	–	2.4	4.6
	65	5.2	4.55	4.65
Experiment 2, column C2, $v = 2.2$	< 0	5.2	4.55	4.65
	0	5.3	–	–
	20	–	2.4	4.6
	65	5.2	4.55	4.65
Experiment 3, column C1, $v = 5.6$	< 0	5.4	5.0	95
	0	5.0	–	–
	20	–	2.6	95
	65	5.7	5.4	95
Experiment 4, column C1, $v = 5.6$	< 0	5.3	5.1	4.7
	0	5.0	–	–
	4.6	–	2.5	4.7
	22.8	5.3	5.1	4.7
Experiment 5, column C2, $v = 0.2$	< 0	5.2	5.4	4.7
	0	5.0	–	–
	4.4	–	2.5	4.7
	20.8	5.2	5.4	4.7
Experiment 6, column C2, $v = 4.9$	< 0	11.5	49	470
	0	3.1	0.62	1.7
	20	11.5	49	470

where CEC is the cation exchange capacity of the adsorbent (in mol_c/kg), z_M is the charge of cation M, and q_M is the amount of cation M adsorbed (in mol/kg). For the ternary Ca^{2+}–Mg^{2+}–Na^+ system, CEC can be expressed as:

$$\mathrm{CEC} = 2\,q_{\mathrm{Ca}} + 2\,q_{\mathrm{Mg}} + q_{\mathrm{Na}} \tag{4}$$

Having defined the activities of adsorbed species as the equivalent fractions y_M, the mass action laws corresponding to Eqs. (1) and (2) for the Gaines–Thomas convention can be written as:

$$K^{\mathrm{GT}}_{\mathrm{NaCa}} = \frac{y^2_{\mathrm{Na}}(a_{\mathrm{Ca}}/c_0)}{y_{\mathrm{Ca}}(a_{\mathrm{Na}}/c_0)^2} \tag{5}$$

$$K^{\mathrm{GT}}_{\mathrm{MgCa}} = \frac{y_{\mathrm{Mg}}(a_{\mathrm{Ca}}/c_0)}{y_{\mathrm{Ca}}(a_{\mathrm{Mg}}/c_0)} \tag{6}$$

where K^{GT} are the Gaines–Thomas exchange coefficients, a_M are the activities of the free metal ions in solution, and c_0 is the reference unit 1 mol/l.

Eqs. (5) and (6) always yield a slope of 1 in a log–log plot of the amount adsorbed versus activity in solution (Vulava et al., 2000). However, experimental slopes are often close to but not equal to unity. In the Rothmund–Kornfeld formulation (Bond, 1995; Rothmund and Kornfeld, 1918; Sposito, 1981) of the Gaines–Thomas exchange convention, the activity of the exchanger species is assumed to be equal to the charge equivalent fraction raised to the power n^{-1}. This formulation offers the flexibility to adjust the slope and vertical displacement of the adsorption isotherms. While some researchers report different exponents for different binary systems (Bond and Verburg, 1997), others applied individual exponents to each cation in their system (Carlson and Buchanan, 1973). In this study, the most simple approach with a unique exponent n^{-1} is used. Raising the charge equivalent fractions to n^{-1} is equivalent to raising the ratio of the activities of the species in solution to the power n:

$$K_{\mathrm{NaCa}}^{\mathrm{RK}} = \frac{y_{\mathrm{Na}}^2}{y_{\mathrm{Ca}}} \left(\frac{(a_{\mathrm{Ca}}/c_0)}{(a_{\mathrm{Na}}/c_0)^2} \right)^n \tag{7}$$

$$K_{\mathrm{MgCa}}^{\mathrm{RK}} = \frac{y_{\mathrm{Mg}}}{y_{\mathrm{Ca}}} \left(\frac{(a_{\mathrm{Ca}}/c_0)}{(a_{\mathrm{Mg}}/c_0)} \right)^n \tag{8}$$

where K^{RK} are the Rothmund–Kornfeld exchange coefficients. For $n = 1$, the Rothmund–Kornfeld formulation and the classical Gaines–Thomas convention are identical. Adsorption isotherm equations for each cation M can be derived by solving Eq. (4) for the respective concentration of the adsorbed species, q_{M}. In a log–log plot, adsorption isotherms resulting from the Gaines–Thomas equation exhibit a slope equal to 1, while isotherms resulting from the Rothmund–Kornfeld equation have a slope equal to n.

The Gaines–Thomas equation is also used in a multi-site approach, in which experimental cation adsorption isotherms are modeled as a linear superposition of adsorption isotherms corresponding to several classes of binding sites with different exchange coefficients. Such a multi-site approach accounts for the heterogeneity of natural soil materials and the nonideality of cation exchange behavior in an empirical fashion (Cernik et al., 1996; Vulava et al., 2000). In multi-site models, the total charge of the cation exchange sites equals the CEC:

$$\sum_i z_i S_i = \mathrm{CEC} \tag{9}$$

where S_i and z_i are the concentration and the charge of site i, respectively.

Solution speciation was included in all model calculations according to the following reactions:

$$\mathrm{Ca^{2+} + Cl^- \leftrightarrows CaCl^+} \quad \log K = 0.57 \tag{10}$$

$$\mathrm{Mg^{2+} + Cl^- \leftrightarrows MgCl^+} \quad \log K = 0.63 \tag{11}$$

$$\mathrm{Na^{+} + Cl^- \leftrightarrows NaCl^0} \quad \log K = -0.19 \tag{12}$$

with thermodynamic stability constants K derived from conditional constants (Martell and Smith, 1982; Smith and Martell, 1989). The Davies equation was used for activity corrections (Sposito, 1981).

The amounts of cations adsorbed were related to the activities of free cations in solution, assuming that adsorption of chloride complexes of Ca and Mg is negligible. The entire ternary dataset was used to fit the 1-GT exchange model using a nonlinear least squares procedure (Cernik and Borkovec, 1995). Subsequently, the 1-GT model was extended to the 1-RK and the 3-GT model, respectively. The fit was optimized by stepwise trial-and-error adjustment of the model parameters. The total charge concentration of exchange sites was set to equal the CEC. Fitting parameters in the 1-GT model were the two exchange coefficients (Eqs. (5) and (6)). In the 1-RK model the parameter n (equaling 1 in Gaines–Thomas convention) was optimized and the exchange coefficients readjusted. In the case of the 3-GT model, two additional sites with very low concentrations were added to the 1-GT model in order to improve the fit of adsorption data in specific regions of the adsorption isotherms. Relative mean square errors (RMSE) were calculated for all fits using the equation:

$$\mathrm{RMSE} = \sqrt{\frac{1}{n}\sum_{i=1}^{n}\left(\frac{\log(q_{i,\mathrm{exp}}/q_0) - \log(q_{i,\mathrm{calc}}/q_0)}{\log(q_{i,\mathrm{exp}}/q_0)}\right)^2} \qquad (13)$$

where $q_{i,\mathrm{exp}}$ and $q_{i,\mathrm{calc}}$ are the measured and the calculated amounts adsorbed of datapoint i, respectively, n is the total number of datapoints, and q_0 is the reference unit 1 mol/kg.

Transport was predicted using a continuous mixing-cell transport code based on a kinetic approach. Solution is assumed to constantly flow through a cascade of stirred mixing cells with instantaneous mixing in each cell. Transport and chemical reactions are directly coupled and the combined differential equations solved simultaneously. While the reactions follow stoichiometrically balanced reaction equations, the respective reaction rates can be defined as a function of activities in solution, i.e., they do not have to follow elementary mass law kinetics. This is necessary if Rothmund–Kornfeld exchange coefficients, which do not depend on the reaction stoichiometry, are used in transport modeling. However, as cation exchange reactions are very fast, reaction rates were chosen high enough to maintain local equilibrium. For the 1-GT model, the same predictions were obtained from the kinetic transport code and from the thermodynamic transport code ECOSAT (Keizer et al., 1993). Input parameters for transport predictions were the sorption model parameters, the soil material packing density, and the column Péclet number.

3. Results and discussion

3.1. Binary cation adsorption

The adsorption data for all binary cation systems are shown in Fig. 1. The data are plotted as adsorbed cation concentrations q_{M} (in mol/kg) as a function of the concentration of free cations M in solution (mol/l). Each figure shows a set of

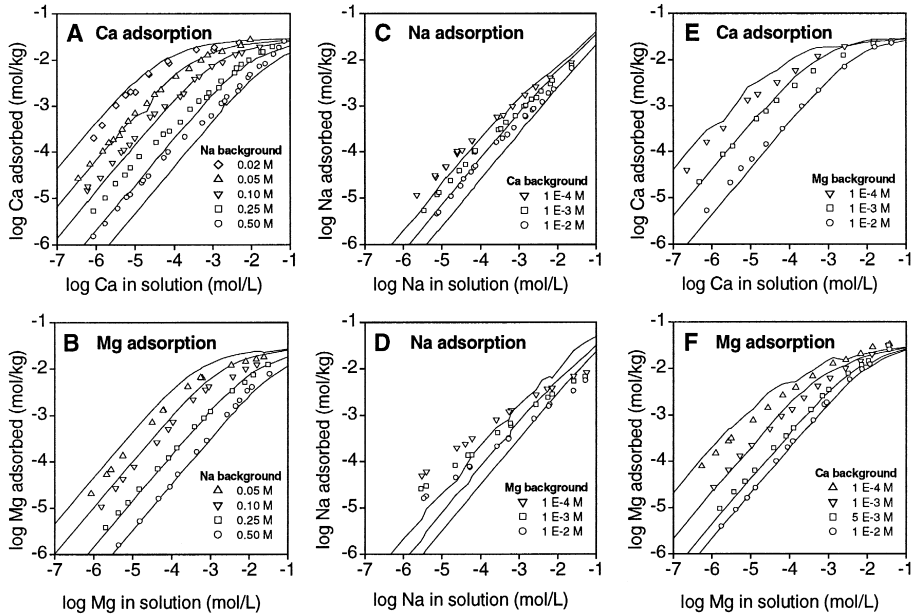

Fig. 1. Binary sorption data (symbols) and 1-site Gaines–Thomas (lines) model fit. Model calculations based on measured final cation concentrations. Background concentrations indicated before addition of the sorbing cation.

adsorption isotherms in the presence of different total concentrations of the respective background cation. Several general features of the adsorption isotherms can be observed: At high adsorptive cation concentrations in solution, the adsorbed amounts approach a plateau value, which corresponds to the CEC of the soil material (0.060 mol_c/kg). At low adsorptive cation concentrations in solution, the experimental adsorption isotherms are linear with a slope near unity on a log–log plot. Due to cation exchange with the background cation, the adsorbed amounts generally decrease with increasing background cation concentration.

The solid lines in Fig. 1 represent the best-fit description of the experimental data with the 1-GT cation exchange model. Model calculations are based on measured final adsorptive and background cation concentrations. The small wiggles in the calculated lines are due to slight variations in measured background cation concentration caused by experimental and analytical errors. This applies also to model calculations presented in Figs. 3 and 4, respectively. Although the model captures the general features of the binary adsorption data rather well, significant deviations from the experimental data still remain, particularly at low adsorptive cation concentrations. The deviations are most apparent in the case of Na adsorption isotherms with Ca or Mg as the background cation. The experimental Na adsorption isotherms at low Na concentrations exhibit a slope of approximately 0.9 and 0.7 in Ca and Mg background electrolyte, respectively. In contrast, a slope of unity follows from the Gaines–Thomas convention of cation exchange (Fig. 1C and D). For Ca and Mg adsorption isotherms with Na as the

background cation, the Gaines–Thomas model provides a rather good description of the experimental data (Fig. 1A). Only at high Na concentration and low Ca concentration the amounts of sorbed Ca are clearly underestimated by the model. The adsorption data for the binary Ca–Mg system are described well by the Gaines–Thomas model (Fig. 1E and F).

The model parameters for the 1-GT model are provided in Table 3. The exchange coefficients indicate that the adsorption affinity to the soil material decreases in the order $Ca^{2+} > Mg^{2+} \gg Na^{+}$. Coefficients for the Riedhof soil are in the same range as values reported by other authors for natural soil materials (Cernik et al., 1994; Dance and Reardon, 1983; Valocchi et al., 1981).

Fig. 2 shows Gaines–Thomas exchange coefficients determined from the individual data points as a function of the respective adsorptive cation concentration in solution and at different background cation concentrations. The constant exchange coefficients used in the 1-GT model are shown as horizontal lines for comparison. While the exchange coefficients for Ca and Mg adsorption remain rather constant with increasing Ca or Mg concentration in solution, the exchange coefficients for Na adsorption increase strongly with decreasing Na concentration. In general, the exchange coefficients seem to increase with increasing concentration of background cations in solution.

Classical exchange isotherms are usually obtained at constant solution normality and, in the case of homovalent exchange, constant ionic strength. In the dataset presented here, ionic strength and solution normality increase with increasing adsorptive cation concentration at a given background electrolyte concentration. However, in the regions of the isotherms where the adsorptive cation concentration is at least 10 times lower than the background cation concentration, solution normality and ionic strength are dominated by the background electrolyte and therefore virtually constant. The presented model calculations implicitly account for complex or ion pair formation in solution and ion activity corrections, which could result in apparent effects of ionic strength on cation exchange. Nevertheless, variations in the calculated selectivity coefficients are observed over the entire range of the adsorption isotherms, but independently of changes in ionic strength. For example, in the case of K_{MgNa}, K_{CaMg}, K_{MgCa}, and K_{CaNa}, the coefficients vary with the background cation concentration, but remain almost constant over the entire adsorptive cation concentration range even at increasing ionic strength. In the case

Table 3
Model parameters for the 1-site Gaines–Thomas model, the 1-site Rothmund–Kornfeld model, and the 3-site Gaines–Thomas model

		$\log K_{NaCa,\,i}$	$\log K_{MgCa,\,i}$	n	$z_i S_I$ ($mmol_c/kg$)	RMSE[a] ($n = 343$)
1-site Gaines–Thomas model		−0.90	−0.16	1	60.0	0.0752
1-site Rothmund–Kornfeld model		−0.84	−0.22	0.94	60.0	0.0660
3-site Gaines–Thomas model	Site 1	−0.90	−0.16	1	60.0	0.0535
	Site 2	5.00	−2.00	1	0.1	
	Site 3	−4.00	−2.00	1	0.1	

[a] RMSE: root mean square error (Eq. (13)).

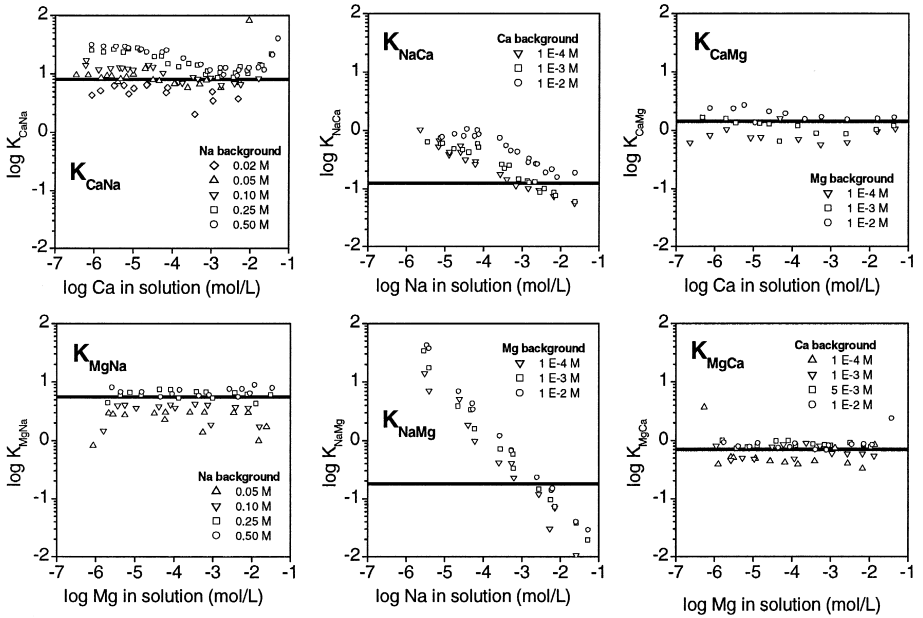

Fig. 2. Exchange coefficients calculated for individual sorption data points (symbols) and binary exchange coefficients from the 1-site Gaines–Thomas model fit (lines). Individual coefficients higher than the model coefficients indicate sorption data points where sorption is underestimated by the 1-site Gaines–Thomas model.

of K_{NaCa} and K_{NaMg}, the selectivity coefficients steadily decrease with increasing Na concentration in solution, even in the regions of constant ionic strength. These results suggest that the observed changes in cation selectivity coefficients are not due to variations in ionic strength and that other factors must be considered.

One explanation might be the nonideality of the exchanger phase, resulting in a variation of activity coefficients for adsorbed cations (Sparks, 1995). In the Gaines–Thomas convention, the activity coefficients for adsorbed cations are assumed to equal 1. The Rothmund–Kornfeld formulation accounts for the variability of the activity coefficients in an empirical fashion: Activities of adsorbed cations are assumed to be equal to the charge equivalent fraction raised to the power n^{-1}. This offers the flexibility to fit the slope of an isotherm more accurately by adjusting the exponent parameter n (Eqs. (7) and (8)). The solid lines in Fig. 3 represent the best-fit description of the experimental data with the Rothmund–Kornfeld model. An isotherm slope $n = 0.94$ together with slightly adjusted exchange coefficients yielded the best fit over all binary datasets. Model parameters are listed in Table 3. Compared to the 1-GT model, the fit of the Na exchange isotherms was slightly improved (Fig. 3C and D), however, at the cost of slightly lower accuracy for the Ca and Mg exchange isotherms (Fig. 3E and F). Furthermore, the slope ($= 0.9$) of the experimental Na adsorption isotherms in Ca background is not the same as the corresponding slope ($= 0.7$) in Mg background electrolyte. The RMSE for the 1-RK model is slightly lower than for the

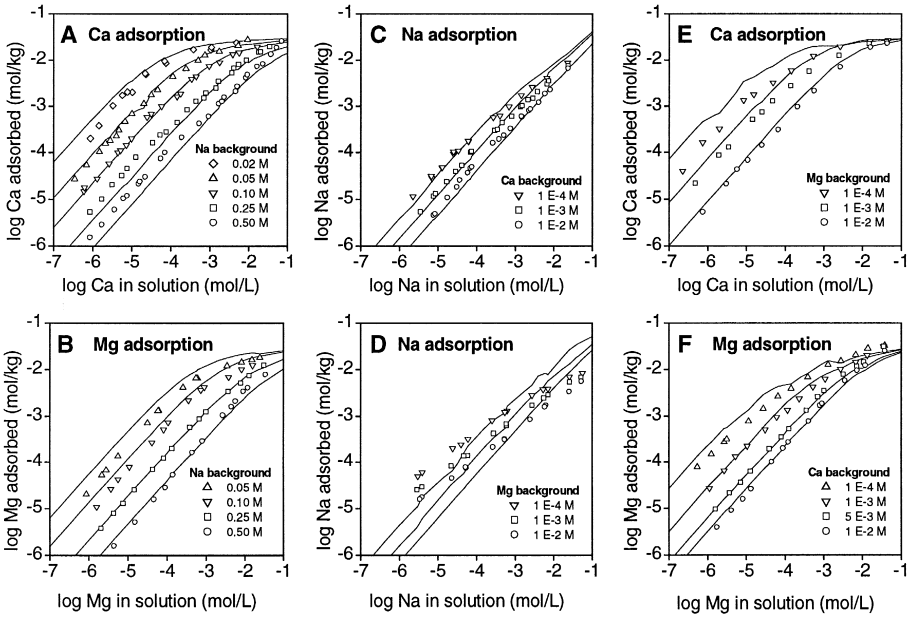

Fig. 3. Binary sorption data (symbols) and 1-site Rothmund–Kornfeld (lines) model fit. Model calculations based on measured final cation concentrations. Background concentrations indicated before addition of the sorbing cation.

1-GT model (Table 3). The Rothmund–Kornfeld formulation is often reported to yield an excellent fit of cation exchange data (Bond, 1995; Carlson and Buchanan, 1973). This was also true in our case if each binary dataset was considered separately (not shown). However, the ability of the Rothmund–Kornfeld approach to improve the simultaneous description of all binary datasets within the Ca–Mg–Na soil system was limited. This was mainly due to the fact that the experimental Na adsorption isotherms exhibited different slopes in Ca and Mg background electrolytes.

It should be noted, however, that we used one unique exponent n in our study, while other researchers used either different exponents for different binary systems (Bond and Verburg, 1997), or applied individual exponents to each cation in their system (Carlson and Buchanan, 1973). Both approaches were also considered in the present study. Using individual exponents for each cation did not further improve the fit, because it offered little additional flexibility to fit different slopes of Na adsorption isotherms in Ca and Mg background electrolytes. The exponent assigned to a cation does not only affect the slope of its model isotherms, but also the vertical displacement of the adsorption isotherms, where the respective cation acts as the background cation. Using a different exponent parameter n for each binary system has the disadvantage that it does not yield a consistent description of the ternary system based on two binary exchange reactions (Eqs. (7) and (8)) and the charge balance (Eq. (4)), without making assumptions on which binary exchange parameters to be considered in the ternary case (Bond and Verburg, 1997).

Another possible reason for the variation in exchange coefficients may be the chemical heterogeneity of the sorbent. Several chemically different surface sites with different concentrations and selectivities for cations could lead to the observed variation in the overall 'macroscopic' exchange coefficients (Fig. 2). The soil material used in this study contains a mixture of different exchanger phases including different clay minerals and soil organic matter. Such chemical heterogeneity can be accounted for in an empirical fashion using the multi-site modeling approach (Cernik and Borkovec, 1995; Cernik et al., 1996; Vulava et al., 2000). To improve the model fit, two additional sites were added to the 1-GT model to account for sites with high affinity for Na and Ca, respectively. The additional model parameters were optimized by trial and error. These two additional sites are hypothetical, however, not unrealistic for a natural soil material. Preferential adsorption of Ca on soil organic matter and of Na on montmorillonitic soil clay has been previously reported (Fletcher et al., 1984a,b; Sposito and Fletcher, 1985). Model parameters and RMSE for the 3-GT model are listed in Table 3. Experimental data (symbols) and model fits (solid lines) are depicted in Fig. 4. The first site was the same as in the 1-GT model. Since the concentrations of the additional two sites did not significantly increase the total site concentration, the concentration of site 1 was left unchanged compared to the 1-GT model. Site 2 accounts for the higher affinity for Na at low Na concentrations. Ca and Mg isotherms are not significantly affected by this site. Comparing Figs. 1 and 4 illustrates that this site significantly improves the fit of the Na adsorption isotherms at low Na concentrations, especially in Ca background electrolyte.

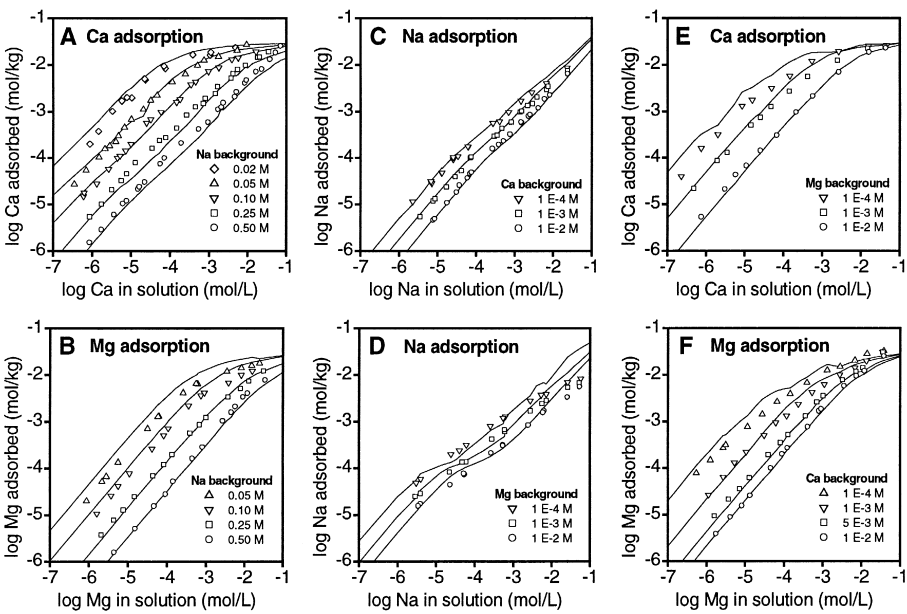

Fig. 4. Binary sorption data (symbols) and 3-site Gaines–Thomas (lines) model fit. Model calculations based on measured final cation concentrations. Background concentrations indicated before addition of the sorbing cation.

However, overestimation of Na adsorption at high Na concentrations is not corrected. This is also not possible by decreasing the Na–Ca exchange coefficient of site 1, since this would lead to an increase in estimated Ca and Mg adsorption in Na background and therefore deteriorate rather than improve the overall fit. Site 3 with a low Na–Ca exchange coefficient improves the fit of Ca adsorption data at high Na concentrations. The effect of this site becomes apparent when comparing Figs. 1A and 4A. For Mg adsorption in Na background and the Ca–Mg system, the 3-GT model did not change the description as compared to the 1-GT model.

3.2. Ternary cation transport

The results of the first two cation transport experiments (Experiments 1 and 2; Table 2) are presented in Fig. 5A. In both experiments, the feed solution was switched three times after the effluent composition had reached a steady state. Experimental results obtained with the two columns (C1 and C2) at different flow velocities are in excellent agreement, indicating that there was no effect of column dimension or flow velocity on the breakthrough behavior of Ca, Mg, and Na. Because Na was present in similar concentrations as Ca and Mg (Table 2), the Na saturation of the cation exchange complex never exceeded 5%. The breakthrough fronts are therefore largely detemined by normality changes and Ca–Mg exchange reactions. The nonretarded normality fronts appear exactly one pore volume after the influent solution was switched, i.e. at 1, 21, and 66 pore volumes. They reflect the changes in total normality of the feed solution. Due to the preference of the exchanger for Ca over Mg, Ca–Mg exchange results in so-called self-sharpening cation exchange fronts observed at around 10 and 71 pore volumes, while the Mg–Ca exchange yields a so-called self-broadening cation exchange front ranging from 30 to 55 pore volumes. Na had only minor effects on the breakthrough pattern: a small combined Ca–Na and Mg–Na exchange shoulder after one pore volume, a Na–Ca exchange front after 21, and a Ca–Na exchange front after 66 pore volumes. Due to low Na adsorption, Na exchange fronts are almost nonretarded and therefore overlap with the normality fronts.

The predictions of the breakthrough curves for Ca, Mg, and Na resulting from the 1-GT and the 1-RK models are shown as solid and dashed lines, respectively (Fig. 5A). The predictions obtained from both models are similar, however with minor deviations in different regions of the transport experiment. Generally, the positions of the exchange fronts are correctly predicted, however, small deviations from the experimental data occur in the diffuse Mg–Ca exchange front.

Predictions from the 3-GT model for experiments 1, 2, and all subsequent transport experiments are not shown. They are virtually identical to those from the 1-GT model. Although the fit of the adsorption data was better with the 3-GT model, these improvements were only at low concentration levels that do not play an important role in the transport experiments.

The influence of Na on the cation breakthrough pattern was much greater in Experiment 3, where the Na concentration in the feed solutions was increased by a factor of 20 (Fig. 5B; Table 2). In this experiment, the Na saturation of the exchanger phase was approximately 40% after column preconditioning and reached almost 65% at

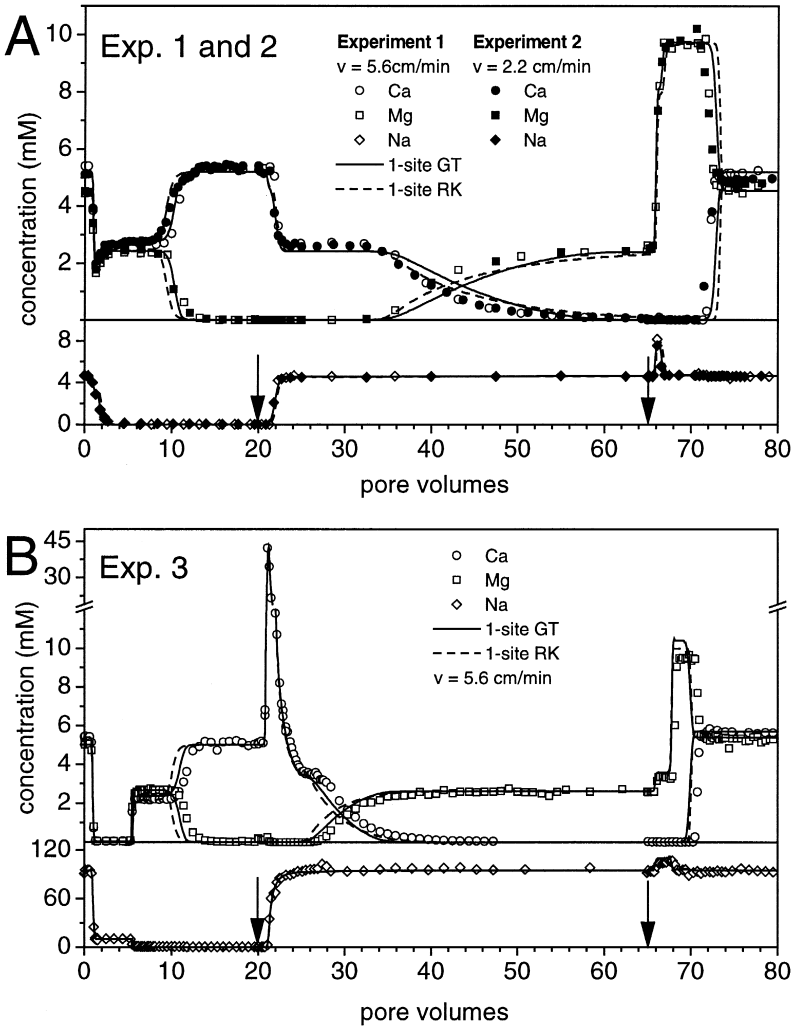

Fig. 5. Results from transport experiments 1–3 (symbols) and model predictions with 1-site Gaines–Thomas (solid lines) and 1-site Rothmund–Kornfeld (dashed lines) model. Experiments 1 and 2 (A) with same solutions. Higher Na concentrations in experiment 3 (B) result in more complex breakthrough curves.

50–65 pore volumes. Thus, all three cations had a strong influence on cation sorption, resulting in a more complex breakthrough pattern. Unretarded normality fronts appear as in Experiments 1 and 2, and also the Ca–Mg and Mg–Ca exchange fronts are the same, though at slightly different positions. The main differences in Experiment 3 are the exchange fronts of Ca and Mg with Na, which are now more pronounced.

The 1-site Gaines–Thomas model yields a rather good prediction of the ternary cation transport behavior, although again minor deviations from the experimental data occur in different regions of the experiment. The 1-RK model yields a similar prediction,

however, slightly less accurate in the region of the Ca–Mg exchange front at 11 pore volumes and the Mg–Ca exchange front around 30 pore volumes.

In Experiments 4 and 5 (Table 2), the situation was further complicated by changing the composition of the feed solution before steady state in the outflow was reached, resulting in overlapping breakthrough fronts. The results of these experiments are depicted in Fig. 6A and B, respectively. Up to an effluent volume of four pore volumes, the breakthrough pattern was similar as described for experiments 1 and 2. Well before the occurrence of the Ca–Mg exchange front, a second change in feed solution composition was applied (Table 2), resulting in a nonretarded normality front combined with a slightly retarded Na front at around five and a half pore volumes. At about 12 pore volumes, the Ca–Mg exchange front originating from the first feed solution change starts to appear in the effluent, but overlaps with the diffuse Mg–Ca exchange front resulting from the second feed solution change. The third change in feed solution composition resulted in additional normality and exchange fronts overlapping with the diffuse Mg–Ca exchange front.

In this case, the model prediction with the Rothmund–Kornfeld model is clearly more accurate than with the Gaines–Thomas model. The complex Ca–Mg exchange front from 12 to 18 pore volumes is accurately predicted with the Rothmund–Kornfeld model. Therefore, also the height of the Ca peak near 24 and 22 pore volumes in experiments 4 and 5, respectively, is predicted more accurately with the 1-site Rothmund–Kornfeld model. However, as the influent was switched twice before steady state was attained, small errors in transport predictions accumulate. With increasing duration of the experiment, predictions become less accurate for both models.

An additional transport experiment (Experiment 6; Table 2) was designed to mimic a seawater–freshwater intrusion system with respect to the concentrations of Ca, Mg, and Na (Beekman and Appelo, 1990; Gomis-Yagües et al., 1997). The experimental results and corresponding model predictions are presented in Fig. 7. Note, that the concentrations are now plotted on a logarithmic scale to better illustrate the concentration changes over wide ranges. The column was preconditioned with a solution in which the cation concentrations resemble seawater. As a result, around 66% of the exchange sites are saturated with Na, 25% with Mg, and only 9% with Ca. Switching to a solution resembling freshwater (at 0 pore volumes) results in a nonretarded normality front at one pore volume. After nine pore volumes, a Mg–Na exchange front appears, followed by a Ca–Mg exchange front at 15 to 20 pore volumes. After equilibrium with "freshwater" has been achieved, about 87% of the exchange sites are occupied with Ca, 12% with Mg, and only about 1% with Na. Switching back to "seawater" at 25 pore volumes again results in a sharp Ca-peak due to the normality front combined with a Na-Ca and subsequent Mg–Ca exchange front.

In this experiment, in which the cation concentrations vary over wide ranges, the 1-GT model provides a slightly better prediction than the 1-RK model. However, both models overestimate the initial amount of adsorbed Na and predict a much sharper Ca–Mg exchange front at around 17 pore volumes than was observed in the experiment. In batch experiments, Sposito and LeVesque (1985) observed a decrease in Ca preference of an exchanger with increasing Na-saturation. This effect leads back to the problem of predicting ternary cation systems based on binary adsorption data.

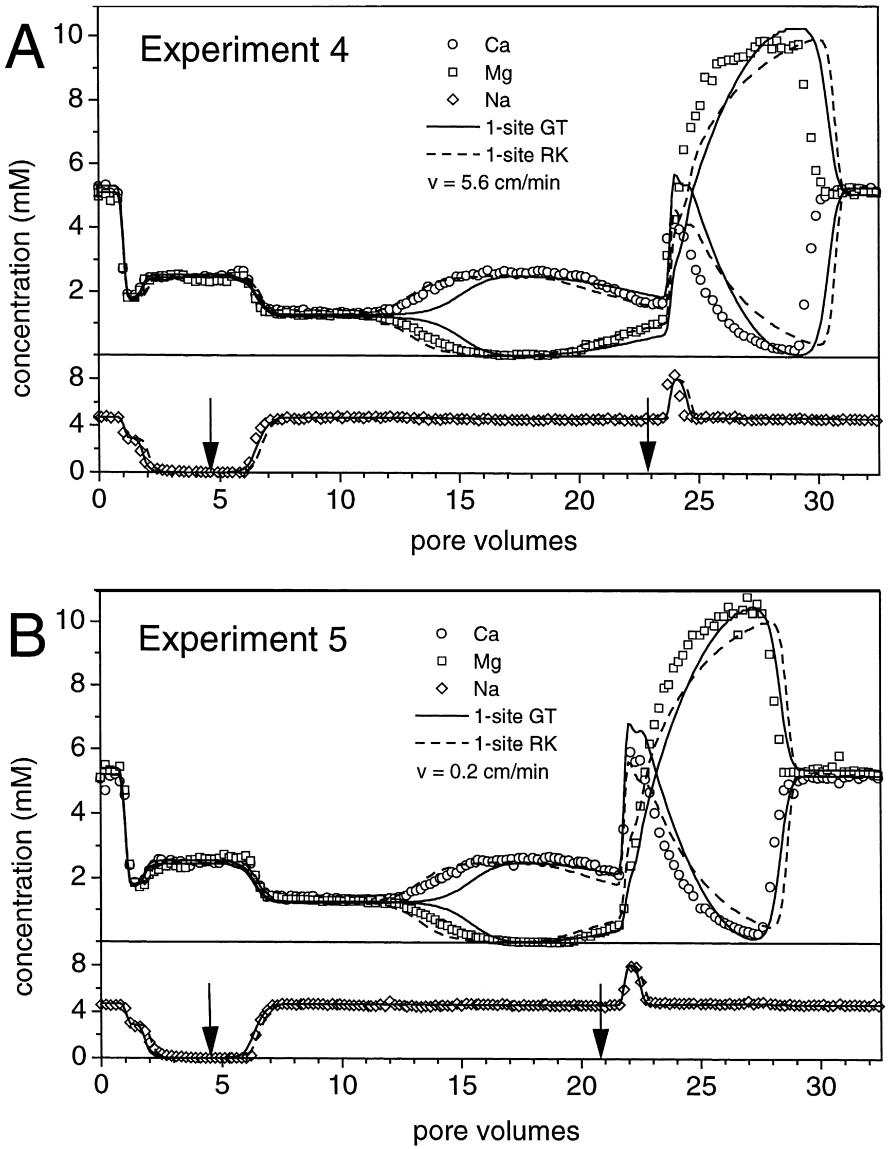

Fig. 6. Results from transport experiments 4 and 5 (symbols) and model predictions with 1-site Gaines–Thomas (solid lines) and 1-site Rothmund–Kornfeld (dashed lines) model. Similar solutions as in experiments 1 and 2. Switching solutions before steady state results in a complex coupled breakthrough pattern with overlapping fronts.

As mentioned earlier, all transport predictions presented in this paper are based on the local equilibrium assumption. To challenge this assumption, the flow velocity was varied from 5.6 cm/h in Experiment 4 to 0.2 cm/h in Experiment 5. Since the model

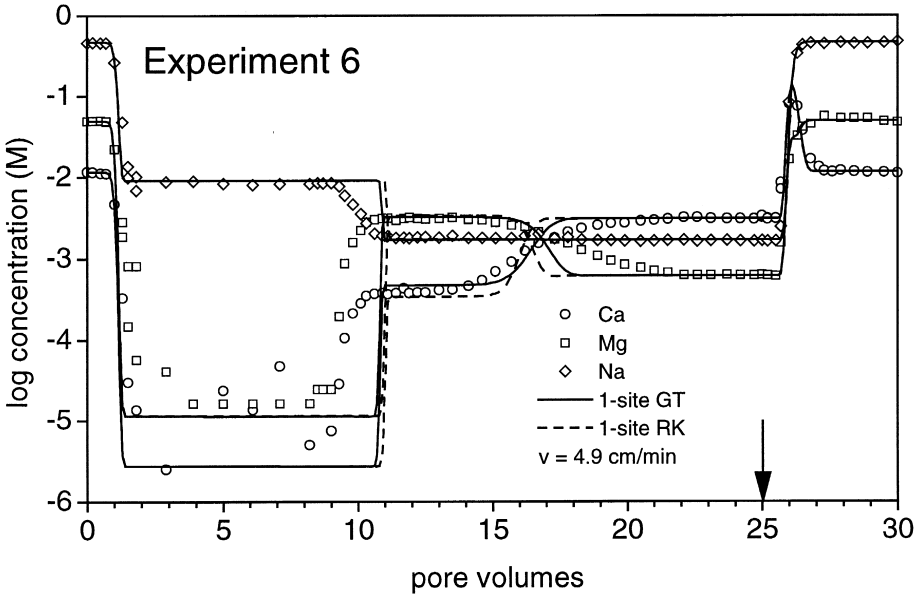

Fig. 7. Results from transport experiment 6 (symbols) and model predictions with 1-site Gaines–Thomas (solid lines) and 1-site Rothmund–Kornfeld (dashed lines) model. Mimicked sea–freshwater intrusion system with respect to typical concentrations of Ca, Mg, and Na.

predictions did not improve with decreasing flow velocity, we conclude that kinetic effects are not responsible for the deviations between model calculations and experimental data. Cation exchange reactions are known to be extremely fast (Sparks, 1995). Furthermore, uniformly packed soil material from a sieve fraction between 63 and 400 μm was used, minimizing physical nonequilibrium effects.

Finally, it is important to stress that the correct determination of the CEC at the condictions of interest is a necessary prerequisite for accurate transport modeling of major cations. For fitting adsorption data shown on a log-scale, an error in the CEC value of up to 20% would not be critical to obtain a good fit. However, transport experiments are usually shown on a linear time scale and the position of exchange fronts depends on the amounts of cations adsorbed. Therefore, special attention should be payed to the determination of the CEC value of the soil material at the pH conditions of interest.

4. Conclusions

Our results demonstrate, that all three models calibrated with binary cation adsorption data for Ca, Mg, and Na are able to predict the general transport behavior in a ternary system of major cations with sufficient accuracy. In principle, this should also be true for more complex systems, containing more than three competing cations. The 1-RK

model slightly improved the fit of the adsorption dataset. However transport predictions were partly improved and partly deteriorated when compared to the 1-GT model. While the 3-GT model provided a better description of Na adsorption in Ca or Mg background than both 1-site models, the transport predictions were virtually the same as for the 1-GT model. This may be explained by the fact that the improvements of the 3-GT model account for adsorption at extremely low adsorptive cation concentrations. In most cases of practical importance, these regions are not decisive for the prediction of the transport patterns of major cations. However, the multisite approach might prove very useful if sorption and transport of trace metal cations at low concentrations are investigated. At the concentration level of major cations that are mainly retained by cation exchange, accurate determination of the CEC at the conditions where transport takes place, is a key prerequisite for accurate transport modeling.

Acknowledgements

This research was funded by the Swiss Ministry of Science and Education, in the framework of EU project FAMEST. Valuable discussions with M. Borkovec and D. Grolimund are greatfully acknowledged.

References

Appelo, C.A.J., Willemsen, A., Beekman, H.E., Griffioen, J., 1990. Geochemical calculations and observations on salt water intrusions: II. Validation of a geochemical model with laboratory experiments. Journal of Hydrology 120, 225–250.

Beekman, H.E., Appelo, C.A.J., 1990. Ion chromatography of fresh- and salt-water displacement: laboratory experiments and multicomponent transport modelling. Journal of Contaminant Hydrology 7, 21–37.

Bjerg, P.L., Christensen, T.H., 1993. A field experiment on cation exchange-affected multicomponent solute transport in a sandy aquifer. Journal of Contaminant Hydrology 12, 269–290.

Bond, W.J., 1995. On the Rothmund–Kornfeld description of cation exchange. Soil Science Society of America Journal 59, 436–443.

Bond, W.J., Verburg, K., 1997. Comparison of methods for predicting ternary exchange from binary isotherms. Soil Science Society of America Journal 61, 444–454.

Carlson, R.M., Buchanan, J.R., 1973. Calcium–magnesium–potassium equilibria in some california soils. Soil Science Society of America Proceedings 37, 851–855.

Cernik, M., Barmettler, K., Grolimund, D., Rohr, W., Borkovec, M., Sticher, H., 1994. Cation transport in natural porous media on laboratory scale: multicomponent effects. Journal of Contaminant Hydrology 16, 319–337.

Cernik, M., Borkovec, M., 1995. Regularized least-squares methods for the calculation of discrete and continuous affinity distributions for heterogeneous sorbents. Environmental Science and Technology 29, 413–425.

Cernik, M., Borkovec, M., Westall, J.C., 1996. Affinity distribution description of competitive ion binding to heterogeneous materials. Langmuir 12, 6127–6137.

Dance, J.T., Reardon, E.J., 1983. Migration of contaminants in groundwater at a landfill: a case study: 5. Cation migration in the dispersion test. Journal of Hydrology 63, 109–130.

Fletcher, P., Holtzclaw, K.M., Jouany, C., Sposito, G., LeVesque, C.S., 1984a. Sodium–calcium–magnesium exchange reactions on a montmorillonitic soil: II. Ternary exchange reactions. Soil Science Society of America Journal 48, 1022–1025.

Fletcher, P., Sposito, G., LeVesque, C.S., 1984b. Sodium–calcium–magnesium exchange reactions on a montmorillonitic soil: I. Binary exchange reactions. Soil Science Society of America Journal 48, 1016–1021.

Gaines, G.L.J., Thomas, H.C., 1953. Adsorption studies on clay minerals. II: A formulation of the thermodynamics of exchange adsorption. The Journal of Chemical Physics 21, 714–718.

Gomis-Yagües, V., Boluda-Botella, N., Ruiz-Beviá, F., 1997. Column displacement experiments to validate hydrogeochemical models of seawater intrusions. Journal of Contaminant Hydrology 29, 81–91.

Grolimund, D., Borkovec, M., Federer, P., Sticher, H., 1995. Measurement of sorption isotherms with flow-through reactors. Environmental Science and Technology 29, 2317–2321.

Hendershot, W.H., Duquette, M., 1986. A simple barium chloride method for determining cation exchange capacity and exchangeable cations. Soil Science Society of America Journal 50, 605–608.

Jury, W.A., Flühler, H., 1992. Transport of chemicals through soil: mechanisms, models, and field applications. Advances in Agronomy 47, 141–201.

Keizer, M.G., De Wit, J.C., Meussen, J.C.L., Bosma, W.J.P., Nederlof, M.M., Venema, P., Meussen, V.C.S., van Riemsdijk, W.H., van der Zee, S.E.A.T.M., 1993. ECOSAT, A Computer Program for the Calculation of Speciation in Soil–water Systems. Wageningen, Netherlands.

Martell, A.E., Smith, R.M. (Eds.), 1982. Critical Stability Constants vol. 5 Plenum, New York.

McBride, M.B., 1994. Environmental Chemistry of Soils. Oxford Univ. Press, New York.

Rothmund, V., Kornfeld, G., 1918. Der Basenaustausch im Permutit I. Zeitschrift für Anorganische und Allgemeine Chemie 103, 129–163.

Smith, R.M., Martell, A.E. (Eds.), 1989. Critical Stability Constants vol. 6. Plenum, New York.

Sparks, D.L., 1995. Environmental Soil Chemistry. Academic Press, San Diego.

Sposito, G., 1981. The Thermodynamics of Soil Solutions. Oxford Univ. Press, New York.

Sposito, G., Fletcher, P., 1985. Sodium–calcium–magnesium exchange reactions on a montmorillonitic soil: III. Calcium–magnesium exchange selectivity. Soil Science Society of America Journal 49, 1160–1163.

Sposito, G., LeVesque, C.S., 1985. Sodium–calcium–magnesium exchange on Silver Hill illite. Soil Science Society of America Journal 49, 1153–1159.

Thomas, G.W., 1982. Exchangeable cations. In: Page, A.L. (Ed.), Methods in Soil Analysis: Part 2 vol. 9 ASA and SSSA.

Valocchi, A.J., Roberts, P.V., Parks, G.A., Steel, R.L., 1981. Simulation of the transport of ion-exchanging solutes using laboratory-determined chemical parameter values. Ground Water 19, 600–607.

Vulava, V.M., Kretzschmar, R., Rusch, U., Grolimund, D., Westall, J.C., Borkovec, M., 2000. Cation competition in a natural subsurface material: modeling of sorption equilibria. Environmental Science and Technology 34, 2149–2155.